Nanoscale

RSC Publishing

PAPER

Metallicity retained by covalent functionalization of graphene with phenyl groups

Cite this: *Nanoscale*, 2013, **5**, 7537

Peizhe Tang,[ab] Pengcheng Chen,[a] Jian Wu,[a] Feiyu Kang,[c] Jia Li,*[c] Angel Rubio*[b] and Wenhui Duan*[ad]

To resolve the controversy over the functionalization effect on conductivity, we systematically investigate the structural and electronic properties of graphene covalently functionalized with phenyl groups. Using first-principles calculations combined with the model Hamiltonian analysis, we find that the structural stability, electronic and transport properties of the functionalized graphene are strongly dependent on the adsorption site of the phenyl groups. In detail, double-side functionalized graphene is energetically more favorable than single-side functionalized graphene, and more importantly, they exhibit an exotic non-magnetic metallic state and a magnetic semiconducting state, respectively. For covalently double-side functionalized graphene, two bands contributed by π electrons of graphene cross at the Fermi level with the preserved electron–hole symmetry, and the Fermi velocity of carriers could be flexibly tuned by changing the coverage of the phenyl groups. These results provide an insight into the experimental observation [*ACS Nano* 2011, **5**, 7945], interpreting the origin of the increase in the conductivity of graphene covalently functionalized with phenyl groups. Our work reveals the great potential of these materials in future nanoelectronics or sensors by controlling the attachment of phenyl groups.

Received 30th March 2013
Accepted 12th June 2013

DOI: 10.1039/c3nr01572f

www.rsc.org/nanoscale

I Introduction

In recent years, graphene has received considerable attention from the scientific community for its potential use as a building block in future nanoelectronic devices,[1–4] due to its high charge-carrier mobility,[5,6] current-carrying capability,[7] and thermal conductivity.[8,9] The lack of a band gap, however, has hampered the applications of graphene, and functionalization has been proposed as a mechanism to introduce a band gap in graphene and bring it into the realm of Si-based electronics.[2,10] On the other hand, the large scale synthesis of graphene under realistic conditions, being extremely important for the real industry, remains a major challenge for scientists.[11–13] Owing to the low cost and easy fabrication processes, chemical solvent-based exfoliation of graphite is regarded as a possible way to overcome this bottleneck.[14–17] During this process, graphene could be covalently functionalized. Recently, a considerable number of experimental works have focused on diazonium salts, which are the reactive reagents and have been used for modification of the surface of sp^2-hybridized carbon materials,[18–21] epitaxial graphene[22,23] and exfoliation graphene.[24–28] It is found that graphene grafting by phenyl groups (specifically, 4-*tert*-butylphenyl groups, TBP)[27] can be achieved through effective reductive activation. Several spectroscopy techniques, for example Raman spectroscopy, atomic force microscopy and high-resolution transmission electron microscopy, have been utilized to identify the phenyl functional groups on the basal plane of graphene.[27]

From the theoretical viewpoint, covalent functionalization of graphene will introduce local defects, leading to some new physics in the Dirac electron system.[29,30] In the honeycomb lattice of graphene, there exist two equivalent sublattices (denoted as A and B). An isolated point modification on sublattice A can induce a quasi-localized virtual bound state (VBS) on the neighboring atoms belonging to sublattice B due to the breaking sublattice symmetry. The wave function of the VBS has three-fold symmetry (D_{3h})[29] and decays as $1/r$ at large distances.[31] The exchange coupling between adjacent point defects can result in the splitting of a VBS to induce ferromagnetism in graphene at certain concentrations of point defects.[32–35] The introduction of a VBS in graphene normally can also open a band gap around the Fermi level; however, the Dirac cones in the graphene may be preserved, depending on the concentration and spatial arrangement of the chemisorbed groups used for chemical functionalization.[36,37]

[a]*Department of Physics and State Key Laboratory of Low-Dimensional Quantum Physics, Tsinghua University, Beijing 100084, People's Republic of China. E-mail: dwh@phys.tsinghua.edu.cn*

[b]*Nano-Bio Spectroscopy Group, Dpto. Física de Materiales, Universidad del País Vasco, Centro de Física de Materiales CSIC-UPV/EHU-MPC and DIPC, Av. Tolosa 72, E-20018 San Sebastián, Spain. E-mail: angel.rubio@ehu.es*

[c]*Engineering Laboratory for Functionalized Carbon Materials, Key Laboratory of Thermal Management Engineering and Materials, Graduate School at Shenzhen, Tsinghua University, Shenzhen 518055, People's Republic of China. E-mail: lijia@phys.tsinghua.edu.cn*

[d]*Institute for Advanced Study, Tsinghua University, Beijing 100084, People's Republic of China*

In experimental situations, the conductivity of graphene with phenyl groups covalently bonded to its basal plane by different functionalization methods was observed to exhibit different behaviors (*i.e.*, enhancement behavior[22,38] and suppression behavior[26] induced by covalent functionalization), which is still under dispute. In addition, room temperature magnetic order has also been found in phenyl-group functionalized graphene nanostructures.[39,40] Therefore, in order to understand experimental observations of functionalized graphene, it is highly desirable to explore possible stable phenyl functionalized structures and the influence of functionalization on the electronic, transport and magnetic properties of graphene, which will be helpful for its use in future nanoelectronics.

In this work, based on the first-principles calculations, we systematically investigate the structural and electronic properties of graphene covalently functionalized with TBP which is taken as a representative of the phenyl groups. We find that the single-side attachment of TBP onto graphene (denoted as s-CFG) can induce a quasi-localized VBS, resulting in the ferromagnetism and gap opening as expected. On the other hand, single-side functionalization can activate the nearest-neighboring carbon atoms next to the adsorption site, and consequently another TBP group can easily adsorb at the activated site on the opposite side to form a more stable structure. Since no breaking of charge conjugation and space-time inversion symmetry occurs, covalently double-side functionalized graphene with TBP (denoted as d-CFG) exhibits an exotic non-magnetic metallic state with two bands crossing at the Fermi level and the preserved electron–hole symmetry. Moreover, the Fermi velocity of carriers is sensitively dependent on the coverage of the phenyl groups. Because the metallic bands are mainly contributed by π electrons of graphene but have little connection with the detailed structure of the phenyl groups, it is anticipated that the metallic state can be present in graphene functionalized with other phenyl groups, such as nitrophenyl groups. Importantly, our two dimensional (2D) quantum transport calculations clearly reveal that s-CFG shows a semiconductor behavior, whereas d-CFG a metallic transport behavior. This can offer an insight towards resolving the controversy of recent experimental transport measurements of graphene functionalized with phenyl groups, and suggest that functionalized graphene can be assembled into various electronic devices by controlling the adsorption of phenyl groups.

II Models and methods

The spin-polarized DFT calculations are performed *via* the Vienna *ab initio* simulation package (VASP).[41] The projector augmented wave (PAW) potential[42] and the generalized gradient approximation with Perdew–Burke–Ernzerhof functional[43] are used to describe the core electrons and the exchange-correlation energy, respectively. The cutoff energy for the plane wave basis set is set to 450 eV. The Brillouin zone is sampled by Monkhorst-Pack k points. The energies are converged to below 10^{-5} eV and the residual forces on all atoms are converged to below 0.01 eV Å^{-1}. A supercell with a vacuum distance of 12 Å normal to the graphene plane is used. The accuracy of our method is benchmarked against a recent study,[44] where the DFT calculations were used to determine the adsorption energy for the attachment of hydrogen atoms onto graphene with the surface coverage of 0.20 nmol cm^{-2}. Our result (-0.77 eV) is the same as their result. The two-dimensional quantum transport properties are adopted *via* Atomic ToolKit package,[45] which combines non-equilibrium Green's function (NEGF) methods with DFT to simulate open systems in a two-probe geometry. Single-ζ polarized atomic basis sets for expanding the electronic density, the local density approximation for exchange–correlation energy, and converged k meshes for the periodic boundary condition perpendicular to the transport direction are all well tested and adopted in the whole calculations.

III Results and discussion

We start by investigating the geometrical structures of s-CFG and find that the interaction between the TBP group and the graphene sheet is quite weak in comparison with that between hydrogen/fluorine and the graphene sheet.[44,46] The adsorption energy (E_{ad}) of attaching one TBP group onto graphene is just -0.29 eV and the zero point energy correction[47] is 11.37 meV. The binding energy is very close to that of an isolated C_6H_5 radical adsorbed onto graphene (-0.25 eV),[48] but the resulting vibrational energy is smaller than that of the oxygen adsorbed onto the metal surface.[47] The weak interaction indicates that s-CFG is not very stable and the TBP group may be easily removed. In the optimized structure, as shown in Fig. 1a, a C–C bond of 1.59 Å is formed between the TBP group and the graphene sheet. Carbon atom A connected to the TBP group is displaced out of the basal plane of the graphene sheet by 0.55 Å, causing a larger bond length between A and B atoms (1.52 Å) than that in the pristine graphene (1.42 Å). Correspondingly, the sp^3 hybridization occurs at the functionalized site, which induces a structural distortion of the graphene sheet. Decreasing the TBP coverage can release the local strain and thus lower the single-side adsorption energy significantly (Fig. 2).

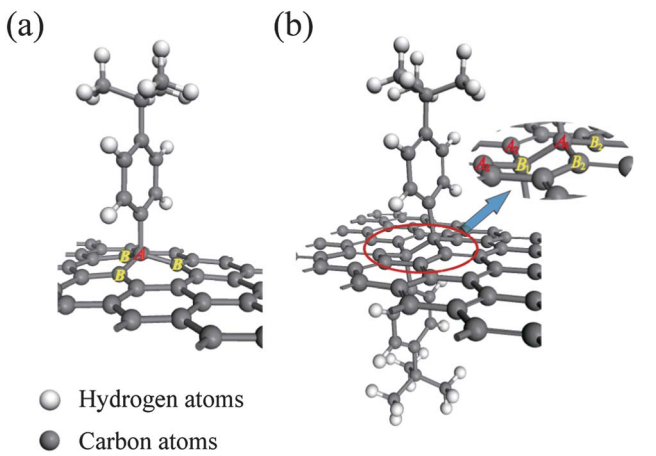

Fig. 1 Optimized geometrical structures of (a) single-side functionalized graphene by TBP groups (s-CFG) and (b) double-side functionalized graphene by TBP groups (d-CFG). The graphene carbon atoms marked A and B belong to different sublattices.

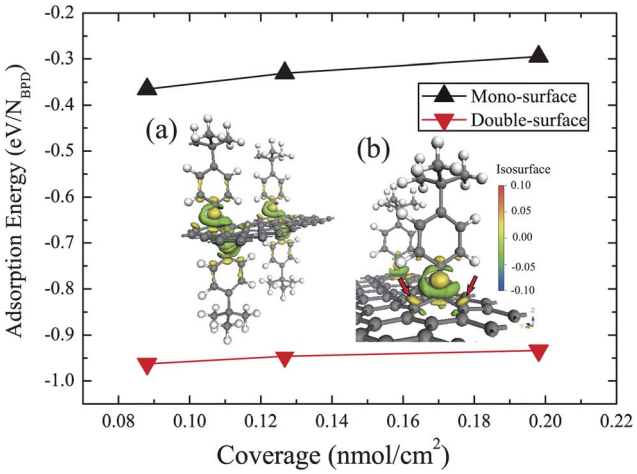

Fig. 2 Calculated adsorption energy per TBP group for different surface coverage and charge density difference (in units of e Å^{-3}) for (a) s-CFG and (b) d-CFG. The red arrows indicate the nearest-neighboring carbon atoms of the attachment site. The adsorption energy E_{ad} is defined as $E_{ad} = (E_{graphene+nTBP} - E_{graphene} - nE_{TBP})/n$, where n is the number of TBP groups.

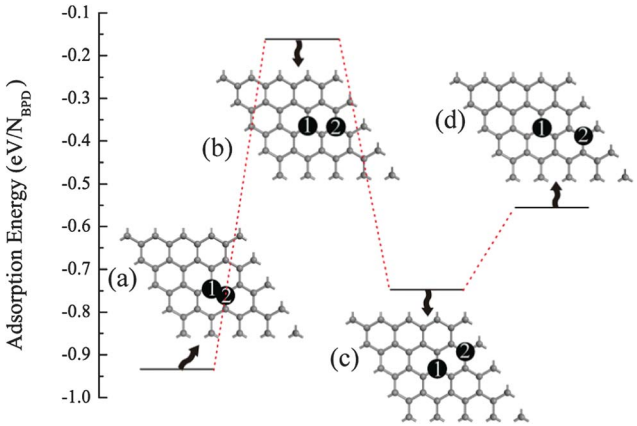

Fig. 3 Adsorption energies for attaching the second TBP group on the opposite side of the graphene sheet in the 4 × 4 supercell model. Four different configurations (a–d: ortho, meta, para, and neighboring ring) of d-CFG are considered, where black circles with numbers 1 and 2 represent the sites for the first and second TBP attachments, respectively.

Since covalent functionalization of graphene with grafted TBP groups can be accomplished from solvent-based exfoliation of graphite, TBP groups may adsorb on both sides of the graphene sheet. To investigate the double-side adsorption, we consider four adsorption sites on the opposite side of the graphene sheet for attaching the second TBP group, as shown in Fig. 3. It can be seen that among all possible binding sites for the second attachment, the ortho position of the graphene ring (Fig. 1b and 3a) is the most energetically favorable site: the adsorption energy E_{ad} for attaching the second TBP group is −0.93 eV, much lower than those of s-CFG (−0.29 eV) and double C_6H_5 radical functionalized graphene sheet (−0.64 eV),[48] indicating that the double-side functionalized graphene with phenyl groups is most likely to form in the experiments.[27] When the second TBP group is attached at the para position (Fig. 3c), the energy is 0.19 eV higher than that of the most stable configuration (Fig. 3a). In contrast, the meta position (Fig. 3b) is the least stable with E_{ad} of −0.16 eV, even higher than that of s-CFG. The energy of the binding site beyond a hexagonal ring of the first attachment, as shown in Fig. 3d, lies in between those of the ortho and meta positions (Fig. 3a and b). It is interesting to see that for the double side adsorption on the same hexagonal ring, the two TBP groups tend to bind to the carbon atoms belonging to different sublattices. This could be well understood by considering the electronic properties of s-CFG shown below. Moreover, the second attachment also enhances the interaction between all TBP groups and the graphene sheet, indicating that the groups can be hardly removed with double-side adsorption.

In the most energetically favorable d-CFG, which has the ortho configuration as shown in Fig. 1b, the bond length between the TBP group and the graphene sheet is 1.60 Å, very close to that of s-CFG (1.59 Å). The lengths of bonds A_1–B_1, A_1–B_2 and A_2–B_1 (also marked in Fig. 1b) are 1.57 Å, 1.51 Å and 1.51 Å respectively. All of them are larger than the C–C sp^2 bond length in pristine graphene (1.42 Å). Similar to s-CFG, the graphene carbon atoms A_1 and B_1 are displaced out of the basal plane of the graphene sheet on opposite sides respectively. Thus, two sp^3 bonds are formed at the nearest-neighboring carbon site. On the other hand, in contrast to the s-CFG, the adsorption energy of d-CFG varies slightly with the coverage, as shown in Fig. 2. This indicates that the formation of sp^3 bonds located on opposite sides of graphene sheet can effectively release the local strain in the vicinity of functionalized carbon sites.

A more detailed understanding of the adsorption behavior could be obtained by analyzing the change of the electronic properties. Fig. 4a and b show, respectively, the majority-spin and minority-spin band structures of s-CFG with the coverage of 0.20 nmol cm^{-2}. Consistent with previous studies,[29,31,33] quasi-localized VBSs (marked as α) around the Fermi level are induced by the breaking of the sublattice symmetry, and consequently, the itinerant (Stoner) magnetism can be induced by the electron exchange interaction in this system. Evidently the splitting of a VBS leads to a ferromagnetic ground state with a magnetic moment of 1 μ_B per attachment site and these properties hardly change with the increase of coverage. This is in agreement with the recent experimental observations of room temperature magnetic order on the phenyl-group functionalized graphene nanostructures.[39,40] Fig. 4d shows the partial charge density distribution of the α band at the K point. Overall, the charge density of the quasi-localized VBS state, which exhibits three-fold symmetry (D_{3h}) and decays very quickly, is mainly concentrated at the graphene carbon atoms belonging to the sublattice different from that of the functionalized carbon site. This charge distribution can activate the relevant graphene carbon atoms to increase the adsorption energy of the additionally attached TBP groups at these sites. In Fig. 2a, we plot the charge density difference of s-CFG. It can be seen that the σ bond is formed between the TBP group and the graphene sheet. Moreover, the charge density around the attachment site is redistributed and the charge of carbon atoms B is more localized than that of pristine graphene. The distorted sp^2 hybridization of carbon atoms around the attachment site and the localization of charge on carbon atoms B make the ortho site

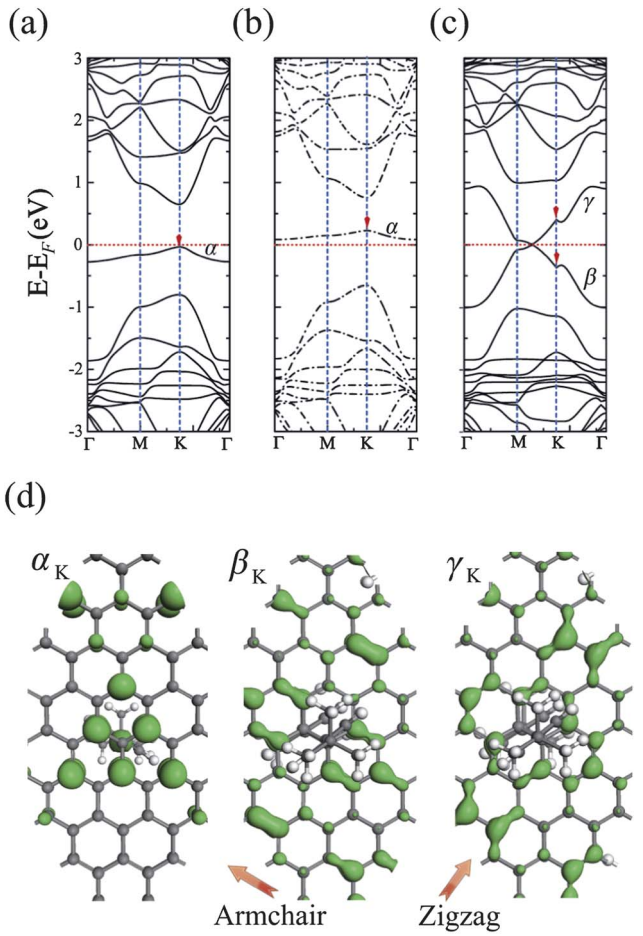

Fig. 4 (a) Majority-spin and (b) minority-spin band structures of s-CFG with the coverage of 0.20 nmol cm^{-2}. (c) Band structure of d-CFG with the coverage of 0.20 nmol cm^{-2}. Fermi levels are set to zero. (d) Isosurfaces of charge density (0.03 e Å^{-3}) of the α, β and γ bands at the K point.

the preferred adsorption site for the attachment of the second TBP group on the opposite side.

Different from the VBS in s-CFG, an exotic nonmagnetic metallic behavior is observed for d-CFG with the coverage of 0.20 nmol cm^{-2}. As shown in Fig. 4c, two dispersive bands (marked as β and γ) with the width of 2 eV cross each other at the Fermi level and the electron–hole symmetry is preserved, similar to the Dirac cone in the pristine graphene. However, the band-crossing point moves from the K point to a nearby *k* point and the Fermi velocity of carriers changes a lot compared with that of the pristine graphene. Toward a better understanding of the physical origin of the metallic bands, we plot the partial charge densities of β and γ bands at the K point in Fig. 4d. It can be seen that the charge of β and γ bands, all contributed by π electrons of graphene, is distributed at the two equivalent sublattices with the twofold symmetry (D_{2h}). Especially, the distribution of charge density of the β band is mainly along the armchair direction of graphene, while that of the γ band is along the zigzag direction (marked by the red arrows in Fig. 4). Moreover, to clarify the relationship between the metallicity of d-CFGs and the coverage of TBP groups, we further calculate the band structures with the different coverage of TBP groups (from 0.09 nmol cm^{-2} to 0.20 nmol cm^{-2}). It is found that the d-CFGs with the different TBP coverages are metallic, but their detailed properties are highly dependent on the coverage of functionalization groups. As shown in Table 1, the Fermi velocity of carriers becomes larger with decreasing coverage of TBP groups and tends to approach the value of the pristine graphene. This indicates that one can significantly modify the electrical conduction properties of d-CFG by changing the coverage of functionalization groups.

Table 1 The Fermi velocity (in units of 10^6 m s^{-1}) of carriers of d-CFGs with different coverages of TBP groups

Structure with coverage	Fermi velocity
d-CFG (0.20 nmol cm^{-2})	0.30
d-CFG (0.13 nmol cm^{-2})	0.53
d-CFG (0.09 nmol cm^{-2})	0.60
Pristine graphene $_{LDA}$[a]	0.85
Pristine graphene $_{GW}$[b]	1.25
Pristine graphene $_{exp}$[a]	1.10

[a] Ref. 49. [b] Ref. 50.

In order to gain further insight into the underlying mechanism of metallicity, a tight-binding Hamiltonian, with nearest-neighbor hopping of p_z electron only, is used to describe d-CFG with the 2 × 2 supercell. In the model, two TBP groups are functionalized at two carbon sites A_1 and B_1 on opposite sides and the Hamiltonian can be written as

$$H = -\gamma_1(a_1^\dagger b_1 + Hc) - \gamma_2\sum_{i>1}^{3}(a_1^\dagger b_i + Hc) - \gamma_2\sum_{i>1}^{3}(a_i^\dagger b_1 + Hc) - \gamma_0\sum_{i>1}^{4}(a_i^\dagger b_i + Hc) \quad (1)$$

where a_i and b_i ($a_i^\dagger$ and $b_i^\dagger$) are annihilations (creations) of a p_z electron on the two different sublattices, respectively. γ_0 is the nearest-neighbor hopping energy in pristine graphene, γ_1 and γ_2 are the projections of hopping energy to the graphene plane between two attachment sites (A_1 and B_1) and from attachment sites to the pristine sites, respectively. In this model, we neglect the energy difference of the p_z electron at different sites. As discussed above, the double-side attachment of two TBP groups results in $\gamma_1 \gg \gamma_0$. Based on the perturbation theory,[51] the effective Hamiltonian of π electrons around the Fermi level (H_{eff}) can be written as

$$\begin{pmatrix} 0 & f_1(\boldsymbol{k}) & 0 & f_2(\boldsymbol{k}) & 0 & f_3(\boldsymbol{k}) \\ f_1(\boldsymbol{k})^\dagger & 0 & f_2(\boldsymbol{k})^\dagger & 0 & f_3(\boldsymbol{k})^\dagger & 0 \\ 0 & f_2(\boldsymbol{k}) & 0 & f_1(\boldsymbol{k}) & 0 & f_4(\boldsymbol{k}) \\ f_2(\boldsymbol{k})^\dagger & 0 & f_1(\boldsymbol{k})^\dagger & 0 & f_4(\boldsymbol{k})^\dagger & 0 \\ 0 & f_3(\boldsymbol{k}) & 0 & f_4(\boldsymbol{k}) & 0 & f_5(\boldsymbol{k}) \\ f_3(\boldsymbol{k})^\dagger & 0 & f_4(\boldsymbol{k})^\dagger & 0 & f_5(\boldsymbol{k})^\dagger & 0 \end{pmatrix} \quad (2)$$

where $f_1(\boldsymbol{k}) = -\gamma_0 e^{i\delta_1\cdot\boldsymbol{k}} + {\gamma_1}^{-1}{\gamma_2}^2 e^{i(-\delta_1\cdot\boldsymbol{k} + 2\delta_2\cdot\boldsymbol{k})}$, $f_2(\boldsymbol{k}) = {\gamma_1}^{-1}{\gamma_2}^2 e^{i(-\delta_1\cdot\boldsymbol{k}+\delta_2\cdot\boldsymbol{k}-\delta_3\cdot\boldsymbol{k})}$, $f_3(\boldsymbol{k}) = -\gamma_0 e^{i\delta_3\cdot\boldsymbol{k}}$, $f_4(\boldsymbol{k}) = -\gamma_0 e^{i\delta_2\cdot\boldsymbol{k}}$, $f_5(\boldsymbol{k}) = -\gamma_0 e^{i\delta_1\cdot\boldsymbol{k}}$, $\boldsymbol{\delta}_1 = \left(\frac{a}{\sqrt{3}}, 0\right)$, $\boldsymbol{\delta}_2 = \left(-\frac{a}{2\sqrt{3}}, -\frac{a}{2}\right)$, $\boldsymbol{\delta}_3 = \left(-\frac{a}{2\sqrt{3}}, \frac{a}{2}\right)$, and a is the lattice constant of pristine graphene. It is found that

H_{eff} satisfies charge conjugation symmetry, which implies $CH_{\text{eff}}C^{\dagger} = -H_{\text{eff}}$, under the charge conjugation operation C and $C^{\dagger}$. Thus the band structure of the d-CFG exhibits electron–hole symmetry, similar to that of pristine graphene. Also, H_{eff} is invariant under the space-time inversion, TI:$H_{\text{eff}} = \sigma_x H^{*}_{\text{eff}} \sigma_x$, where σ_x is the Pauli matrix. Therefore, the band crossing of π and π^{*} states exists at the Fermi level,[52] but different from the pristine graphene it is not at the K point.[53] This fact is in agreement with the results of the first-principles calculations. By analyzing the effective Hamiltonian, we can find that only the matrix elements $f_1(\boldsymbol{k})$ and $f_2(\boldsymbol{k})$ are influenced by the attachment of groups, while the other matrix elements retain their original forms. Therefore, with the decrease of the coverage, the influence of the functionalization groups is suppressed, and the electronic properties of d-CFG should converge to those of pristine graphene when the coverage is small enough. This also coincides with the observation from the first-principles calculations.

The quantum transport properties of the s-CFG, d-CFG and pristine graphene are further calculated to demonstrate the intrinsic overall effects of the periodical covalent functionalization of graphene by using non-equilibrium Green's function (NEGF) methods combined with the density functional theory (DFT) calculations in the generalized gradient approximation. Fig. 5 shows the calculated current–voltage (I–V) curves both for s-CFG and d-CFG with the coverage of 0.20 nmol cm^{-2}. Evidently, the s-CFG exhibits semiconducting behavior as the current is negligible when the bias voltage is smaller than 0.4 V. On the other hand, a metallic transport behavior can be observed for the d-CFG, which is mainly contributed by the π electrons of the graphene sheet.[54] These observations suggest that d-CFG has great potential as a conducting layer and s-CFG can be used as a TBP sensor. At the same voltage, the current of d-CFG with the coverage of 0.20 nmol cm^{-2} is about one third of that in the pristine graphene, and this ratio is in line with that of Fermi velocities between the d-CFG and pristine graphene (shown in Table 1). Therefore, the current in d-CFG could be flexibly tuned by changing the TBP coverage which links with the Fermi velocity in the quantum transport region. This provides an effective method to manipulate the metallicity of d-CFG, and reveals its promising potential in the future nanoelectronics.

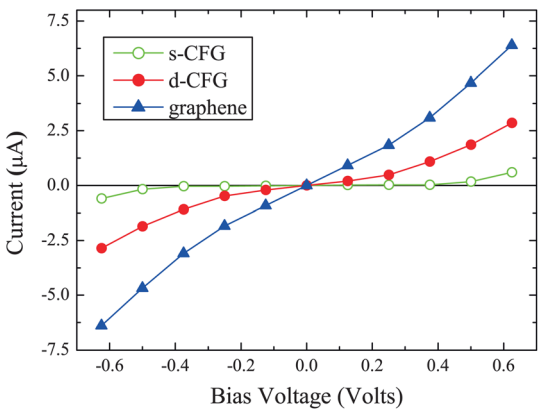

Fig. 5 Current–voltage characteristics of s-CFG, d-CFG and the pristine graphene. The length of the scattering region is ~9 nm.

The above analysis indicates that the metallicity of d-CFG mainly originates from π electrons of graphene, while having little connection with the detailed structure of TBP groups. It is thus that one may expect a universal metallic behavior for graphene functionalized with other phenyl groups. Recent experiments have shown that nitrophenyl groups can be covalently bonded to the graphene basal plane, resulting in a superlattice microstructure of the functionalized graphene, as manifested by atomic force microscopy, transmission electron microscopy and selected area electron diffraction.[28] We thus further calculate the electronic properties of graphene with double-side attachment of nitrophenyl groups. A similar band structure to that of d-CFG functionalized with TBP is observed, but with a difference in the Fermi velocity of carriers.[55] Recent Raman spectroscopy and electric transport measurements by Huang *et al.*[26] showed that CFG functionalized with nitrophenyl groups exhibits good metallic behavior, with conductivity as high as that of exfoliated graphene. Since the samples were synthesized in solution,[26] nitrophenyl groups can be attached to both sides of the graphene sheet, resulting in a metallic behavior as predicted from our calculations. In contrast, if the phenyl groups are chemically adsorbed onto the exfoliated graphene sheet supported by the substrate to lead to single-side attachment, the transport measurement showed a semiconducting behavior.[22,38] The agreement between all of these experimental observations and our theoretical predictions indicates that the electronic properties of CFG are sensitive to the fabrication process and the chemical functionalized graphene with high conductivity can be achieved by controlling the coverage elaborately. This finding provides a flexible method to control the electronic properties of graphene *via* chemical functionalization.

IV Conclusions

The structural and electronic properties of graphene covalently functionalized by TBP groups are investigated using first-principles calculations. The s-CFG exhibits a quasi-localized VBS, which can open a band gap and induce ferromagnetism in graphene as expected. The quasi-localized VBS also activates the nearest-neighboring atoms next to the attachment site, leading to the attachment of another TBP group on the opposite side of graphene. In the d-CFG, two bands (π and π^{*} states) cross each other at the Fermi level and the electron–hole symmetry is preserved, which can be qualitatively understood *via* a tight-binding model Hamiltonian analysis. The transport properties can be flexibly tuned by changing the TBP coverage. The quantum transport calculations show that the s-CFG exhibits a semiconducting behavior, whereas the d-CFG a metallic transport behavior, which are consistent with the band structure calculations. Since the two crossing bands have little connection with the detailed structure of the TBP group, the metallic behavior can also occur in CFG functionalized by other phenyl groups, such as nitrophenyl groups, as confirmed by our further calculations. This may provide an explicit mechanism to resolve the controversy of recent conductivity measurements of graphene functionalized with phenyl groups. Our work also suggests that functionalized graphene can be assembled into

various electronic devices by controlling the attachment of the phenyl group, which may have potential applications as a chemical sensor and a conducting layer.

Acknowledgements

We acknowledge the support of the Ministry of Science and Technology of China (grant no. 2011CB606405 and 2011CB921901), the National Natural Science Foundation of China (grant no. 11074139, 11104155 and 51232005), and the Shenzhen Projects for Basic Research (no. JC201105201119A and JCYJ20120831165730910). AR acknowledges financial support from the European Research Council Advanced Grant DYNamo (ERC-2010-AdG-Proposal no. 267374), Spanish Grants (FIS2011-65702-C02-01 and PIB2010US-00652), Grupos Consolidados UPV/EHU del Gobierno Vasco and European Commission project CRONOS (280879-2 CRONOS CP-FP7).

References

1 A. K. Geim and K. S. Novoselov, *Nat. Mater.*, 2007, **6**, 183–191.
2 M. Allen, V. Tung and R. Kaner, *Chem. Rev.*, 2010, **110**, 132–145.
3 M. S. Fuhrer, C. N. Lau and A. H. MacDonald, *MRS Bull.*, 2010, **35**, 289–295.
4 Q. Yan, B. Huang, J. Yu, F. Zheng, J. Zang, J. Wu, B.-L. Gu, F. Liu and W. H. Duan, *Nano Lett.*, 2007, **7**, 1469–1473.
5 K. I. Bolotin, K. J. Sikes, Z. Jiang, M. Klima, G. Fudenberg, J. Hone, P. Kim and H. L. Stormer, *Solid State Commun.*, 2008, **146**, 351–355.
6 S. V. Morozov, K. S. Novoselov, M. I. Katsnelson, F. Schedin, D. C. Elias, J. A. Jaszczak and A. K. Geim, *Phys. Rev. Lett.*, 2008, **100**, 016602.
7 J. Moser, A. Barreiro and A. Bachtold, *Appl. Phys. Lett.*, 2007, **91**, 163513.
8 A. A. Balandin, S. Ghosh, W. Bao, I. Calizo, D. Teweldebrhan, F. Miao and C. N. Lau, *Nano Lett.*, 2008, **8**, 902–907.
9 Y. Xu, X. B. Chen, J. S. Wang, B. L. Gu and W. H. Duan, *Phys. Rev. B: Condens. Matter Mater. Phys.*, 2010, **81**, 195425.
10 P. C. Chen, Y. C. Li, C. Si, J. Wu, J. Ihm and W. H. Duan, *Appl. Phys. Lett.*, 2012, **101**, 033105.
11 C. Soldano, A. Mahmood and E. Dujardin, *Carbon*, 2010, **48**, 2127–2150.
12 J. Hass, W. A. de Heer and E. H. Conrad, *J. Phys.: Condens. Matter*, 2008, **20**, 323202.
13 J. Wintterlin and M. L. Bocquet, *Surf. Sci.*, 2009, **603**, 1841–1852.
14 X. Cui, C. Z. Zhang, R. Hao and Y. L. Hou, *Nanoscale*, 2011, **3**, 2118–2126.
15 J. M. Englert, J. Roehrl, C. D. Schmidt, R. Graupner, M. Hundhausen, F. Hauke and A. Hirsch, *Adv. Mater.*, 2009, **21**, 4265–4269.
16 Y. Hernandez, V. Nicolosi, M. Lotya, F. M. Blighe, Z. Sun, S. De, I. T. McGovern, B. Holland, M. Byrne, Y. K. Gun'Ko, *et al.*, *Nat. Nanotechnol.*, 2008, **3**, 563–568.
17 J. R. Lomeda, C. D. Doyle, D. V. Kosynkin, W.-F. Hwang and J. M. Tour, *J. Am. Chem. Soc.*, 2008, **130**, 16201–16206.
18 M. Delamar, R. Hitmi, J. Pinson and J. M. Saveant, *J. Am. Chem. Soc.*, 1992, **114**, 5883–5884.
19 Y. C. Liu and R. L. McCreery, *J. Am. Chem. Soc.*, 1995, **117**, 11254–11259.
20 J. L. Bahr, J. Yang, D. V. Kosynkin, M. J. Bronikowski, R. E. Smalley and J. M. Tour, *J. Am. Chem. Soc.*, 2001, **123**, 6536–6542.
21 M. Wu, X. Wu, Y. Gao and X. C. Zeng, *Appl. Phys.Lett.*, 2009, **94**, 223111.
22 E. Bekyarova, M. E. Itkis, P. Ramesh, C. Berger, M. Sprinkle, W. A. de Heer and R. C. Haddon, *J. Am. Chem. Soc.*, 2009, **131**, 1336–1337.
23 L. M. Zhang, J. Yu, M. M. Yang, Q. Xie, H. L. Peng and Z. F. Liu, *Nat. Commun.*, 2013, **4**, 1443.
24 S. Niyogi, E. Bekyarova, M. E. Itkis, H. Zhang, K. Shepperd, J. Hicks, M. Sprinkle, C. Berger, C. N. Lau, W. A. de Heer, E. H. Conrad and R. C. Haddon, *Nano Lett.*, 2010, **10**, 4061–4066.
25 H. Zhang, E. Bekyarova, J.-W. Huang, Z. Zhao, W. Z. Bao, F. L. Wang, R. C. Haddon and C. N. Lau, *Nano Lett.*, 2011, **11**, 4047–4051.
26 P. Huang, H. R. Zhu, L. Jing, Y. L. Zhao and X. Y. Gao, *ACS Nano*, 2011, **5**, 7945–7949.
27 J. M. Englert, C. Dotzer, G. Yang, M. Schmid, C. Papp, J. M. Gottfried, H.-P. Steinrück, E. Spiecker, F. Hauke and A. Hirsch, *Nat. Chem.*, 2011, **3**, 279–286.
28 H. Zhu, P. Huang, L. Jing, T. Zuo, Y. L. Zhao and X. Y. Gao, *J. Mater. Chem.*, 2012, **22**, 2063–2068.
29 T. O. Wehling, A. V. Balatsky, M. I. Katsnelson, A. I. Lichtenstein, K. Scharnberg and R. Wiesendanger, *Phys. Rev. B: Condens. Matter Mater. Phys.*, 2007, **75**, 125425.
30 J. M. García-Lastra, K. S. Thygesen, M. Strange and A. Rubio, *Phys. Rev. Lett.*, 2008, **101**, 236806.
31 C. Bena and S. A. Kivelson, *Phys. Rev. B: Condens. Matter Mater. Phys.*, 2005, **72**, 125432.
32 V. K. Dugaev, V. I. Litvinov and J. Barnas, *Phys. Rev. B: Condens. Matter Mater. Phys.*, 2006, **74**, 224438.
33 O. V. Yazyev and L. Helm, *Phys. Rev. B: Condens. Matter Mater. Phys.*, 2007, **75**, 125408.
34 B. Uchoa, V. N. Kotov, N. M. R. Peres and A. H. Castro Neto, *Phys. Rev. Lett.*, 2008, **101**, 026805.
35 P. Lu, R. Zhou, W. Guo and X. C. Zeng, *J. Phys. Chem. C*, 2012, **116**, 13722–13730.
36 J. M. García-Lastra, *Phys. Rev. B: Condens. Matter Mater. Phys.*, 2010, **82**, 235418.
37 A. R. Muniz and D. Maroudas, *J. Appl. Phys.*, 2012, **111**, 043513.
38 A. Sinitskii, A. Dimiev, D. A. Corley, A. A. Fursina, D. V. Kosynkin and J. M. Tour, *ACS Nano*, 2010, **4**, 1949–1954.
39 J. Hong, S. Niyogi, E. Bekyarova, M. E. Itkis, P. Ramesh, N. Amos, D. Litvinov, C. Berger, W. A. de Heer, S. Khizroev and R. C. Haddon, *Small*, 2011, **7**, 1175–1180.
40 J. Hong, E. Bekyarova, P. Liang, W. A. de Heer, D. C. Haddon and S. Khizroev, *Sci. Rep.*, 2012, **2**, 624.
41 G. Kresse and J. Furthmüller, *Phys. Rev. B: Condens. Matter Mater. Phys.*, 1996, **54**, 11169–11186.
42 G. Kresse and D. Joubert, *Phys. Rev. B: Condens. Matter Mater. Phys.*, 1999, **59**, 1758–1775.

43 J. Perdew, K. Burke and M. Ernzerhof, *Phys. Rev. Lett.*, 1996, **77**, 3865–3868.
44 Ž. Šljivančanin, M. Andersen, L. Hornekęr and B. Hammer, *Phys. Rev. B: Condens. Matter Mater. Phys.*, 2011, **83**, 205426.
45 J. Taylor, H. Guo and J. Wang, *Phys. Rev. B: Condens. Matter Mater. Phys.*, 2001, **63**, 245407.
46 D. W. Boukhvalov and M. I. Katsnelson, *J. Phys.: Condens. Matter*, 2009, **21**, 344205.
47 W. X. Li, C. Stampfl and M. Scheffler, *Phys. Rev. B: Condens. Matter Mater. Phys.*, 2002, **65**, 075407.
48 D. Jiang, B. G. Sumpter and S. Dai, *J. Phys. Chem. B*, 2006, **110**, 23628–23632.
49 D. A. Siegel, C. H. Park, C. Hwang, J. Deslippe, A. F. Fedorov, S. G. Louie and A. Lanzara, *Proc. Natl. Acad. Sci. U. S. A.*, 2011, **108**, 11365.
50 C. Attaccalite and A. Rubio, *Phys. Status Solidi B*, 2009, **246**, 2523–2526.
51 P. A. Lödin, *J. Chem. Phys.*, 1951, **19**, 1396.M.
52 J. L. Mañes, F. Guinea and M. A. Vozmediano, *Phys. Rev. B: Condens. Matter Mater. Phys.*, 2007, **75**, 155424.
53 The determinant of H_{eff} is the product of its eigenvalues. So the solution of the equation $\text{Det}[H_{\text{eff}}] = 0$ determines the band crossing point around the Fermi level. In this case, the solution exists and depends on the specific parameters. So the band crossing here can be observed and is not at the K point, which is consistent with DFT calculations.
54 It should be noted that the electron–phonon (el–ph) coupling might play an important role in the transport properties of some systems. The el–ph coupling, however, will not change the semiconducting transport behavior of s-CFG with a calculated transport gap of 0.8 eV, since the magnitude of reducing gap by el–ph coupling is about tens of meV for carbon materials [V. Perebeinos, J. Tersoff, and P. Avouris, *Phys. Rev. Lett.* 2005, **94**, 086802]. Moreover, the nature of metallic transport of d-CFG will not be changed by the el–ph coupling, which only leads to a renormalization of the Fermi velocity[49] and electron mobility [A. Akturk and N. Goldsman, *J. App. Phys.*, 2008, **103**, 053702] for graphene.
55 The electronic property of d-CFG attached by nitrophenyl groups with a 2×2 supercell is also investigated. However, a small 2×2 supercell (corresponding to high coverage of functional groups) is not suitable for d-CFG since there is no enough space to accompany the close-by methyl groups which belong to different TBP groups. In this case, owing to the small size of the supercell, the attachment of nitrophenyl groups makes the planar graphene sheet distorted strongly and the sp^2 bonding among graphene carbon atoms without nitrophenyl group attachment cannot be kept. So this distortion can break the symmetry of the graphene lattice and strongly affect the electronic properties, resulting in a small band gap (around 0.1 eV).